Sustainable Energy, Grids and Networks 34 (2023) 101048

Contents lists available at ScienceDirect

Sustainable Energy, Grids and Networks

journal homepage: www.elsevier.com/locate/segan

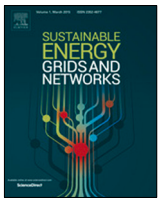

Grey-box modeling for hot-spot temperature prediction of oil-immersed transformers in power distribution networks

E.M.V. Blomgren [a,*], F. D'Ettorre [a], O. Samuelsson [b], M. Banaei [a], R. Ebrahimy [a], M.E. Rasmussen [a], N.H. Nielsen [a], A.R. Larsen [a], H. Madsen [a]

[a] Technical University of Denmark, Department of Applied Mathematics and Computer Science, Lyngby, Denmark
[b] Lund University, Faculty of Engineering, Industrial Electrical Engineering and Automation, Lund, Sweden

ARTICLE INFO

Article history:
Received 25 October 2022
Received in revised form 21 February 2023
Accepted 15 April 2023
Available online 21 April 2023

Keywords:
Grey-box modeling
Dynamic transformer rating
Distribution grid flexibility
Thermal model
Data-driven modeling

ABSTRACT

Power transformers are one of the most costly assets in power grids. Due to increasing electricity demand and levels of distributed generation, they are more and more often loaded above their rated limits. Transformer ratings are traditionally set as static limits, set in a controlled environment with conservative margins. Through dynamic transformer rating, the rating is instead adapted to the actual working conditions of the transformers. This can help distribution system operators (DSOs) to unlock unused capacity and postpone costly grid investments. To this end, real-time information of the transformer operating conditions, and in particular of its hot-spot and oil temperature, is required. This work proposes a grey-box model that can be used for online estimation and forecasting of the transformer temperature. It relies on a limited set of non-intrusive measurements and was developed using experimental data from a DSO in Jutland, Denmark. The thermal model has proven to be able to predict the temperature of the transformers with a high accuracy and low computational time, which is particularly relevant for online applications. With a six-hour prediction horizon the mean average error was 0.4–0.6 °C. By choosing a stochastic data-driven modeling approach we can also provide prediction intervals and account for the uncertainty.

1. Introduction

The decarbonization pathways towards a carbon-neutral Europe are deeply reshaping the power system. Increasing levels of distributed generation (DG) together with the electrification of the heating and transport sectors (e.g. use of heat pumps and electric vehicles) enable a shift from passive to active distribution grids. The increased peaks and congestion that come with the increasing demand have resulted in transformers being more frequently loaded above their rated limits, i.e. nameplate ratings. The overloading could reduce their life expectancy, and also jeopardize the reliability of the entire network. This highlights the need for more dynamic grid operations.

Over the past decades, capacity expansion and replacement of existing grid assets have been the main measures taken by distribution system operators (DSOs) to keep the network running smoothly, while handling an increasing number of new connections and increasing levels of DG and low-carbon technologies (e.g. heat pumps). However, the traditional "connect and reinforce" operating model is economically and environmentally costly and takes time to implement. As a result, new methods to increase transformer capacity, while limiting their aging are needed to reduce the need for expensive network upgrades.

Power transformers are one of the most expensive assets in a power grid infrastructure [1]. Loading a transformer beyond its nameplate capacity increases the leakage flux to the core and outside, which heats the metallic parts of the transformer. This might further affect the internal thermal dynamics as the composition of the insulation oil might change and gas content increase [2]. As a consequence of the transformer losses (i.e. ohmic winding, core and stray losses), the temperature increases. If the transformer hot-spot (the area with the highest temperature) and oil temperature rise above the recommended thermal limits (given by manufacturer or see e.g. [2]), it could increase the insulation's aging rate and reduce transformer lifetime [1].

These limits vary according to the transformer type and cooling strategy. According to IEEE Std. C57.12.00–2015 the average and maximum (hottest-spot) winding temperature rise above ambient temperature shall not exceed 65 °C and 80 °C, respectively, at rated kVA when tested in accordance with IEEE Std. C57.12.90 (i.e. continuous ambient temperature of 40 °C for air-cooled transformers and of 30 °C for water-cooled transformers) [3]. However, such constant conditions are quite unusual

* Correspondence to: Technical University of Denmark DTU, Department of Applied Mathematics and Computer Science, Anker Engelunds Vej 1, 2800, Kongens Lyngby, Denmark.
E-mail address: emvb@dtu.dk (E.M.V. Blomgren).

https://doi.org/10.1016/j.segan.2023.101048

during normal operation [4], as the environment within which the transformer is operated constantly changes. When the ambient temperature is lower than the rated temperature, a higher load can be allowed without increasing the transformer aging rate. Therefore, by adapting the transformer rating to its actual working conditions (i.e. dynamic rating), it is possible to unlock extra capacity, without violation of the safety margins [5], and achieve monetary saving by deferring the investment in new transformers. This strategy is especially useful in colder climates, since the peak demand coincides with low temperatures [6].

The application of dynamic ratings requires increased awareness of the transformer operating conditions to safely increase the load above the nameplate rating, without increasing the risk of failures and safety breaches [7]. More specifically, it requires information on the critical temperatures within the transformer, namely winding, inner core and other metallic hot-spot temperatures as well as top oil temperature. For normal cyclic loading, i.e. normal daily operation, the maximum recommended temperatures are 120 °C, 130 °C, 140 °C and 105 °C, respectively [2]. These temperatures can be either monitored by fiber optics or estimated using transformer thermal models.

The International Electrotechnical Commission (IEC) Standard 60076-7 [2] proposes two different calculation methods for the transformer hot-spot temperature: an exponential equation and a difference equation method. Both methods provide the hot-spot temperature for arbitrarily time-varying load factor and ambient temperature. However, the former method is more suited to be used by manufacturers during tests for the determination of the transformer heat transfer parameters, while the latter method is more suitable for real time monitoring.

In [8], the IEC Std. 60076-7 thermal model was used for dynamic transformer rating for wind energy applications. The model was applied to an existing transformer to assess its reduction in lifespan and reliability when overloaded, and on that basis to provide design and financial considerations. Results showed that by applying dynamic transformer rating, the transformer size can be safely reduced (−20%), thus reducing future investment costs, or that the wind farm can be expanded up to 60%.

In [7], Jalal et al. proposed an extended version of the calculation methods proposed in [2], by developing a dynamic rating algorithm which also includes measurements of the top oil temperature, tap position, and cooling operation in the evaluation of the transformer hot-spot temperature and reduction in lifespan of the insulation.

Similarly, in [9], the differential approach of the IEC Std. 60076-7 was modified to incorporate the dependency of oil viscosity and winding loss on temperature. The proposed improved model was then validated using temperature measurements from a 40 MVA, 21/115 kV, oil forced air forced (OFAF) transformer. Results showed that the improved model outperformed the thermal model proposed by the IEC Std. 60076-7 in estimating the hot-spot temperature for short-time dynamic loading.

Also Annex G of the IEEE C57.91 Standard provides a thermal model that takes in to account the effects on transformer losses of temperature and oil viscosity. However, the requirement of complex and many input parameters is a downside of the methods that rely on the above-mentioned standards, as it complicates the practical implementation. In view of this, simplified models have been proposed as an alternative to the standards' calculation methods.

Arabul and Senol [10] proposed a regression model for hot-spot temperature calculation based on experimental measurements from fiber optic temperature sensors, while aiming to reduce the error rate without increasing input data. Results showed that the proposed method provided more accurate lifetime calculations, by significantly reducing the error in the reduction in lifespan estimation.

Gezegin et al. [11] used both IEC Std. 60076-7 and Annex G of the IEEE C57.91 Standard to develop a new method for average winding and hot-spot temperature, which outperformed the standard methods in their laboratory testing setup.

A further aspect affecting the transformer hot-spot temperature is the presence of harmonic conditions caused by nonlinear loads [12]. In [13], Das et al. proposed an extension of the two IEC Std. 60076-7 thermal models that account for unbalanced loading with different harmonic distortions in each phase. The model was then incorporated into a dynamic transformer rating algorithm to help utilities to minimize the risk of transformer failure.

A 3-D finite element model was used by Huang et al. [14] to investigate the impacts of harmonics on the magnetic flux leakage and hot-spot temperature rise. Simulation results showed that high-order harmonics can produce a hot-spot temperature rise of around 7 °C. A similar approach was used in [15] for evaluating the transformer losses and estimating the lifetime of oil-filled and dry-type transformers under harmonic loads. Based on numerical simulation, Zhang et al. [16] identified a quantitative relationship for the winding temperature rise under different harmonic content and harmonic frequency. As in [14], their results showed that the hot-spot temperature increases from 0.3 °C to 18.7 °C when the harmonic content increases from 1% to 10%.

While the works above focused on the development of thermal models for real-time monitoring and reduction in lifespan estimation, only a few works in the literature turned their attention on thermal models for dynamic rating applications with predictive capabilities. For dynamic rating applications, predictions are a crucial requirement.

Juarez-Balderas et al. [17] developed a prediction model for forecasting the transformer hot-spot temperature based on Artificial Neural Networks (ANN). The model was validated with both finite element method (FEM) simulations and experimental data, and showed accurate prediction with respect to the latter (average error of 2.71%). However, the model was developed for medium voltage/low voltage (MV/LV) transformers and tested indoors. The model thereby does not consider ambient temperature, while using many inputs and computationally heavy FEM calculations. Therefore, the model has little applicability to many small MV/LV transformers placed outdoors. Moreover, the prediction horizon is not reported in the paper, further limiting the applicability to dynamic operation.

Unlike [17], Bracale et al. [18] proposed a probabilistic stress–strength framework to predict the probability of load not exceeding the transformer rating, and formulated an alarm-setting strategy based on this probability. However, the proposed model only detects the transformer status, i.e. either overload or not, but does not provide any quantitative information regarding the overloaded status of the transformer. Thus, the model is not well suited for real-time monitoring and predictions to be used by a grid operator in a dynamic operation setting. Sun et al. [19] used a support vector regression method to predict the hot spot temperature of a distribution grid transformer. The input data for the method includes the ambient temperature, load rate, historical hot spot temperature and cooling fan status. While the simulations results shows high accuracy of results, its implementation requires hot spot temperature data and can be applied only to the dry-type transformers.

Rommel et al. [20] proposed a method to predict hot spot temperature of transformers when limited information is available. The method uses voltage and current measurement to estimate losses and proposed a simple virtual twin of the transformer to estimate the winding hot spot temperature. The virtual twin is created based on only the transformer nameplate data. The method does not consider the impacts of ambient temperature and environmental data such as solar radiation on the results.

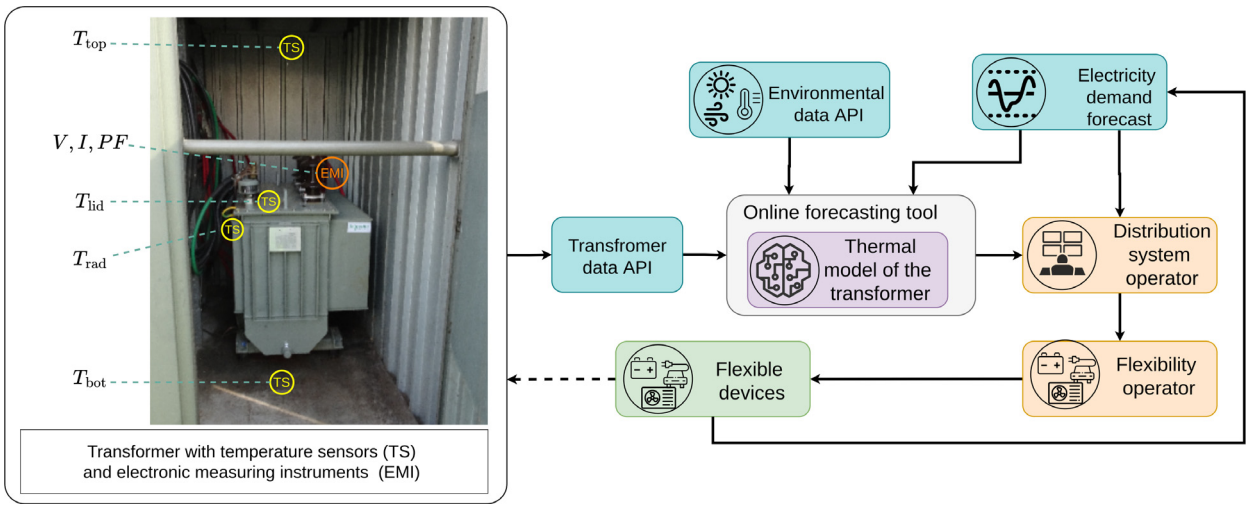

Fig. 1. The proposed general framework of data transactions (solid arrow) and changed power flow (dotted arrow) for dynamic rating of transformers considering flexible devices.

Zhang et al. [21] developed a prediction model for transformer winding hot-spot temperature fluctuation based on fuzzy information granulation and the chaotic particle swarm optimized wavelet neural network. The model shows a high prediction accuracy, but the author suggests more research to make it more applicable to engineering practices.

In this context, the transformer winding hot-spot temperature has been rarely studied for time series prediction [21]. In particular, stochastic models for distribution transformer temperature forecasting which take into account prediction of future disturbances have to date rarely been investigated. To fill this gap, the present paper focuses on presenting a methodology to develop a transformer thermal model for temperature prediction by using stochastic grey-box modeling. The main contribution of this paper is the development of a thermal model for transformers in power distribution grids. The novelties are summarized as follows: The proposed model:

- can provide both estimations and k–step ahead predictions. Hence, the model can be used for online forecasting, and for enabling dynamic rating of distribution grid transformers.
- uses a grey-box modeling approach, meaning that the model accounts for the physics informed and stochastic behavior in the system. This results in the ability to estimate the uncertainty in the predictions and laying the ground for a risk informed dynamic control strategy.
- was developed considering input data accessible through non-intrusive measurements and a model selection process that minimizes the amount of input data (and sensors) was chosen. Thus, the installation required to apply the model for online forecasting is practical and affordable for existing transformers in service.

Furthermore, the proposed model is developed based on experimental data collected during field-trials in the context of the Flexible Energy Denmark (FED) project [22]. This gives the opportunity to investigate and evaluate the transformer temperature predictions in a real world scenario.

The rest of this paper is structured as follows: Section 2 defines the problem and describes the framework within which the thermal model will be applied. Next, Section 3 presents the experimental setup and data acquisition. Section 4 describes the grey-box modeling approach and Section 5 presents and discusses the results. Section 6 concludes the paper.

2. Model application framework

The use of dynamic transformer ratings can help DSOs to unlock extra capacity at distribution grid level and postpone costly grid investments. The dynamic rating should be set relative to the temperature of the transformer, which is the actual limiting factor for the power flow through the transformer. If the temperature is below the thermal limit, a higher power transmission can be allowed. If instead the temperature is above the limit, less power has to be transmitted to avoid transformer failure and aging.

Fig. 1 shows the proposed operational framework of a temperature-based dynamic transformer rating (DTR). In this framework, temperature sensors and power measurement devices monitor the transformer operating conditions. An online forecasting tool fetches the data from the transformer sensors as well as the latest environmental data and load forecasts through APIs. In the online forecasting tool the data is then fed to the thermal model, giving predictions of the transformer temperature in a requested time horizon. The DSO can use these predictions along with load forecasts to determine whether more or less power can be transmitted. The adjustments in power flow could be done through activation of flexible resources. In such a scenario, the DSO could request flexibility from a flexibility operator (for example an aggregator or other actor in a flexibility market). However, determining how this should be done is not within the scope of this work. Through the activation of flexible resources the power flow is changed, and will be visible in the transformer data collected by the online forecasting tool. The electricity demand forecasts are also updated accordingly and the procedure is repeated for each time step.

Successful implementation of this framework requires accurate prediction of the transformer temperature. The goal of this paper is to develop a thermal model that can be used for both parameter and state estimations as well as predictions of the transformer temperature in the online forecasting tool. According to the transformer manufacturer, monitoring the transformer lid temperature is sufficient for avoiding critical overloading conditions as it relates to the top oil temperature. Hence, the proposed model will be used to predict the lid temperature of the transformers. For this purpose we chose the approach of grey-box modeling. Why this approach is chosen and how it is applied is further explained in Section 4.

To develop a model that can be seamlessly applied in the framework of dynamic rating, we aim to find input variables

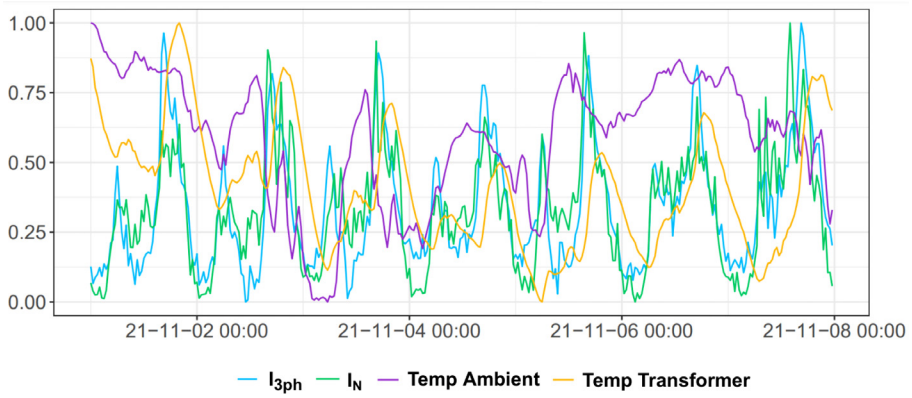

Fig. 2. Example of normalized time series data for three-phase current (I_{3ph}), neutral current (I_N) ambient temperature and transformer temperature, measured on the lid. The data has been filtered to a 30 min time resolution.

that can be measured in a non-intrusive way or that can easily be fetched using existing APIs. Nevertheless, the input variables should be chosen such that acceptable prediction results are obtained. This should result in a solution that is affordable and practical, not requiring any interruption in power delivery or replacement of grid equipment, which has clear economic and environmental benefits.

3. Experimental setup and data acquisition

The installation setup includes two 3-phase 10/0.4 kV oil cooled transformers at two separate low voltage (LV) grids owned by a Danish DSO in Jutland. Both transformers are situated in living labs (LLs) [23] in the Flexible Energy Denmark project [22], meaning they are real world grids that are used for testing new technologies. Transformer 1 (TRF 1) is rated at 400 kVA and serves around 170 residential customers. Transformer 2 (TRF 2) is rated at 200 kVA and serves around 140 residential customers and a small industry. Each transformer supplies 5–10 customers with electric vehicles (EVs) and 15–20 customers with photovoltaic (PV) panels. Heating occurs through a mixture of heat pumps and district heating. The peak load of both transformers is in the range of 200 to 250 kVA. TRF 2 has a relatively larger base load, compared to TRF 1, which could be due to the industrial load. The transformers are installed in ventilated metal housings that are placed outdoors.

Electrical metering devices (EMDs) are installed in a non-intrusive way (i.e. magnetic mounting and clamp-on current/voltage sensors) on the low-voltage side of the two transformers to collect current, voltage, harmonic and power factor data. Four temperature sensors are installed inside the metal housing as shown in Fig. 1. Two sensors measure the housing temperature 10–20 cm below the ceiling (T_{top}) and 10–20 cm above the floor (T_{bot}), while the other two measure the temperatures of the lid of the transformer case (T_{lid}) and of the transformer radiator (T_{rad}). Table 1 summarizes all the measured data.

Thus, the solution is practically simple and can take place without any interruption in power delivery. A sampling rate of one second was used; however, measurements can be filtered to other resolutions considering the mean value of the per second values. The data from the measuring devices is from a third party company, and we fetch the data using an API.

The ambient temperature, wind speed, wind direction and solar radiation data are retrieved from the open data provided by the Danish Meteorological Institute (DMI open data) [24]. All the data is available at 10 min resolution and can be filtered for other resolutions, e.g. 30 min resolution, by considering the appropriate mean value of the 10 min measurements.

Table 1
Measured input variables.

Variable	Notation	Unit
Solar radiation	Gh	W/m^2
Wind speed	Φ_{wind}	m/s
Wind speed South	$\Phi_{wind,S}$	m/s
Wind speed North	$\Phi_{wind,N}$	m/s
Wind speed East	$\Phi_{wind,E}$	m/s
Wind speed West	$\Phi_{wind,W}$	m/s
Ambient temperature	T_a	°C
Transformer lid temperature	T_{lid}	°C
Transformer radiator temperature	T_{rad}	°C
Housing top temperature	T_{top}	°C
Housing bottom temperature	T_{bot}	°C
Apparent three-phase power	S_{3ph}	VA
Phase current	I_{ph}	A
Neutral current	I_N	A

The entire data set available is from November 2021 to June 2022. However, if using the entire data set, there would be seasonal effects in the data that the model would need to describe, for instance annual variations of the solar radiation. To properly describe such seasonal effects we would need a minimum of two years of data and associated parameters estimated with the data at hand will be unreliable. As an initial step of the model development we thus choose a shorter time period, namely November 2021, and thereby we can neglect the seasonal effects. A similar approach is seen in e.g. [25]. An example of the time series data for November 1st 2021 to November 8th 2021 is shown in Fig. 2. The data has been filtered to 30 min time resolution and this resolution is also used in the model development. This time resolution was chosen as a compromise between smooth data where behavior in a longer time scale is seen (typically systems with high inertia) and a more volatile data set where variation in a shorter time resolution is seen (typically systems with low inertia). It is seen in the figure that the peak in transformer temperature generally occurs after peaks in the other data inputs. For the model development, the data set was divided into a training and a testing data set. The training data set is roughly 80% of the entire data set.

4. Modeling approach

The present section describes the stochastic grey-box modeling approach used to develop the thermal model. Grey-box models are introduced first, together with the related mathematical framework, followed by a presentation of model structure and the tested models. Statistical methods are used in the model selection.

4.1. Grey-box modeling

Grey-box models have proven to be an effective way to model the dynamics of complex thermal systems [26]. As their name suggests, grey-box approaches are at the intersection between white box approaches, where the model is derived from the theoretical knowledge of the systems (e.g. continuity, momentum and energy equations), and black box approaches, where statistics, and hence information from data, is used to identify the relationship between the model inputs and outputs, without exploiting any knowledge of its internal process. In grey-box models, the theoretical knowledge of the system is used to suggest a first proposal for the model structure, i.e. a set of first-order stochastic differential equations. Grey-box models are also data-driven in the sense that statistics and input data is used to optimize the parameters of the model [27]. The models are usually written in a continuous-discrete time state-space representation with system equation and observation equation as follows:

$$d\boldsymbol{x}_t = \boldsymbol{A}\boldsymbol{x}_t dt + \boldsymbol{B}\boldsymbol{u}_t dt + \boldsymbol{\sigma} d\boldsymbol{w}_t \tag{1}$$

$$\boldsymbol{y}_k = \boldsymbol{C}\boldsymbol{x}_k + \boldsymbol{e}_k \tag{2}$$

where k are points in time, t_k, of measurements, $\mathbf{x} \in \mathbb{R}^n$ is the state vector, $\mathbf{u} \in \mathbb{R}^p$ is the input vector, $\mathbf{A} \in \mathbb{R}^{n\times n}$, $\mathbf{B} \in \mathbb{R}^{n\times p}$ and $\mathbf{C} \in \mathbb{R}^{m\times n}$ are the state-space matrices, $\mathbf{y} \in \mathbb{R}^m$ is the vector of measured outputs, $\boldsymbol{w}$ are standard Wiener processes with incremental covariance matrix $\boldsymbol{\sigma} \in \mathbb{R}^{n\times n}$, and $\mathbf{e} \in \mathbb{R}^m$ are the measurement errors, each assumed to be Gaussian white noise $\mathcal{N}(0, \sigma_{e_k}^2)$ to the kth measured output. We also assume that the measurement errors for the different measurements are uncorrelated. In this work we assume that the Wiener processes are independent, and thus, the diagonal covariance matrix consists of the corresponding variances, σ_i^2, to each ith Wiener process. Finally, we assume that the Wiener processes and the measurement error are independent.

In this work, an iterative model-selection strategy similar to that described by Bacher and Madsen in [26] was adopted to identify the best dynamic model to estimate and predict the transformer temperature. It consists in a forward selection procedure that starts from the simplest model structure, and then iteratively extends the model by adding new states and/or input variables. Model parameters are found by maximizing the joint probability of the observed data given the model structure (see [28] for a detailed discussion). This was done by using the R-package CTSM-R [27], which is a tool for developing stochastic state space models in R. Given the maximum likelihood estimates of the model parameters, each model was then evaluated by analyzing the corresponding residual auto-correlation function (ACF) and cumulated periodogram to verify the model assumption of white noise residuals. If the residuals are not white noise this reflects that the model does not describe all the systematic variation in the data, and hence the model has to be expanded. Moreover, the visual inspection of the inputs, outputs, and residuals time series was used to detect what effects the model did not capture, and hence to provide insights for the subsequent model extension. Through the expansion of the model, the significance levels of the estimated parameters were also evaluated, aiming for a p-value lower than 5%. If higher p-values were detected, the model was reduced.

Since the transformers considered in this study are located in two different geographical areas and present different loading conditions, as discussed in Section 3, two different models have been investigated.

4.2. Model structure: Transformer heat balance

The model structure was derived from the first law of thermodynamics. By considering the transformer as a closed system that exchanges energy with its surroundings, i.e. external environment, the dynamics of the transformer temperature directly follow from the transformer heat balance:

$$CdT(t) = \Phi_{\text{gain}}(t)dt - \Phi_{\text{loss}}(t)dt \tag{3}$$

where C and T are the transformer thermal capacity and temperature, respectively, Φ_{gain} is the internal heat gains due to the transformer power losses, and Φ_{loss} is the heat losses towards the surrounding environment, such as those due to convective heat transfer between the transformer case and external air. Power losses are due to the dissipative effects that take place within the transformer, i.e. load and no-load losses, further described in 4.2.1. Heat losses towards the environment account for the heat removed by the transformer cooling system, and the convective and radiative heat transfer between the transformer and its surroundings, namely the environment inside the metal housing. Since the latter is affected by outdoor conditions, the impact of local weather data on the transformer temperature was also taken into account. Fig. 3 shows the correlation analysis among the measured variables (Table 1). It can be seen clearly that the transformer temperature is correlated to the external environmental conditions, thus confirming the rationale behind the inclusion of ambient temperature, wind speed and global solar radiation in the modeling process. This also agrees with the IEC Std. 60076-7, stating that environmental factors have a larger impact on smaller transformers, however, the factors are not included in the standard calculation methods [2]. A positive correlation can be noted between the transformer and ambient temperatures: a lower T_a helps to cool down the transformer, while a higher T_a reduces the temperature difference driving the heat transfer, hence the cooling capacity. Conversely, the wind speed and solar radiation input data are inversely correlated to the measurements of T_{lid} (this data behavior and interpretation in terms of the physical system is further discussed in Section 4.2.2).

4.2.1. Transformer power losses

The no-load losses in the transformer are due to the induced voltage in the core. Since the voltage generally has much lower variance than the current, we assumed that the no-load losses are constant in the transformer. Thereby, we simply modeled the no-load losses as a constant, $\Phi_{\text{NL}} = b$.

Load losses on the other hand depend on the increased load as:

$$\Phi_{\text{LL}} = P + \Phi_{\text{EC}} + \Phi_{\text{OSL}} \tag{4}$$

where P, Φ_{EC} and Φ_{OSL} represent ohmic (I^2R), winding eddy current, and other stray losses respectively [29]. All of these losses increase as the total current squared increases. In the thermal model we used only one parameter to model the effect from the current squared. By this formulation, we assumed that the contribution from all parameters, such as impedance or separate effects in (4), can be summarized to one parameter, a ($\Phi_{\text{LL}} \propto aI_{3\text{ph}}^2$).

Moreover, the neutral current will also contribute to the losses and therefore the temperature of the transformer [29,30]. The neutral current is linked to the unbalance between the phases and the third order harmonic components of the phase currents, because of the 120 degree symmetry between the phases [31]. In the data collected from the experimental setup it was seen that the third order harmonic at 150 Hz was the second most apparent frequency component for the three phase currents, while it was

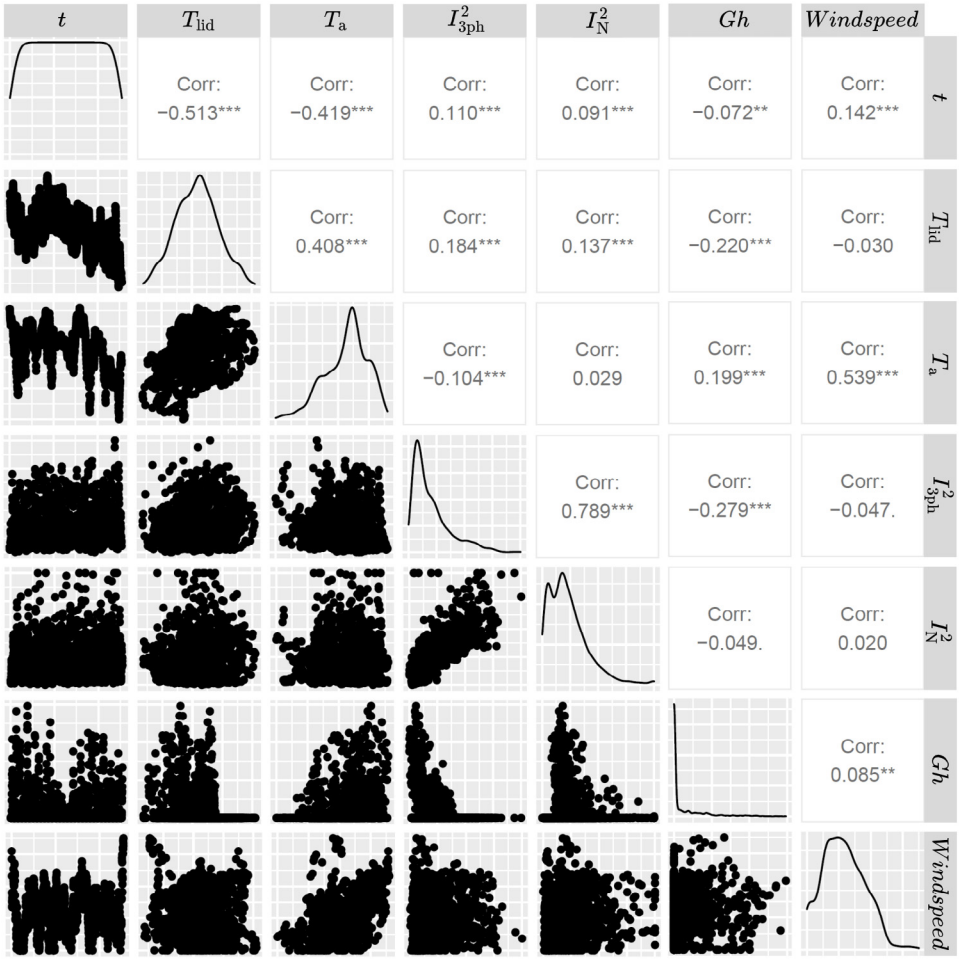

Fig. 3. Scatter plots, correlation and data density distribution using data from TRF 1 from November 2021. Here T_{lid} is the transformer lid temperature, T_a is ambient temperature, I^2_{3ph} is three-phase current squared, I^2_N is neutral current squared and Gh is solar radiation.

the most apparent in the neutral current. The neutral current squared was therefore used as a variable to describe losses related to both third order harmonics as well as unbalanced currents ($\Phi_{LL} \propto cI^2_N$).

In summary, the thermal losses of the transformer can be represented as a function of three-phase current squared and neutral current squared representing the load losses and a constant term representing the no load losses as follows:

$$\Phi_h = \Phi_{LL} + \Phi_{NL} = aI^2_{3ph} + b + cI^2_N \tag{5}$$

4.2.2. Environmental factors

The main environmental factors that were taken into account in the thermal model are ambient temperature, wind and solar radiation.

The wind should have a cooling effect on the housing in which the transformer is placed, but could also cause an increase in temperature if it blocks any ventilation in the housing. Thus, we allowed the parameters for wind to be both positive and negative. Both wind speed and wind direction can potentially affect the thermal model. Investigations showed that including wind direction in the model did not give significant parameters while increasing the size of the model. Hence, it was proposed to model the wind using only one input variable, i.e., wind speed.

The solar radiation should have a heating effect on the housing, indirectly resulting in impacts on the heat convection between the temperature in the housing and the temperature of the transformer. This implies less cooling from the surrounding environment and increased transformer temperature. Fig. 3 shows no indication of linear dependence between solar radiation and transformer temperature. Nevertheless, there could be a dynamic relation between the variables and therefore, another approach was taken to find a suitable solution to model the solar impact.

The impacts of solar radiation can vary over the day due to the change in solar azimuth angle or shadow effects from, for example, buildings or trees. B-splines is a non-parametric method that can be used to model the impact of solar radiation on for instance a building in a data-driven approach [32]. Here, B-splines were used to a model the indirect effect of solar radiation on the transformer temperature, through the heating of the cable cabinets. For further details on the aspects of solar gain modeling using B-splines, the reader is referred to [32]. The B-splines were applied such that they depend on the time of the day, i.e. the sun position. To reduce the model and avoid unnecessary parameters, the B-splines were designed to be active only during the time intervals for which there is solar radiation, i.e. hours 7 to 16. After applying the B-splines to the model it was discovered that the solar radiation had a significant impact on the temperature of both transformers only between hours 7 to 12. Hence, the interval was reduced to these hours. Using B-splines, the estimated solar radiation impact, Φ_{sol}, can be formulated as below:

$$\Phi_{sol}(t) = \sum_{j=1}^{n} sc_j B_j(t) Gh(t) \tag{6}$$

where B_j is the jth spline, $\hat{sc}_j$ is the corresponding estimated parameter to the jth spline and Gh is the solar radiation. Since the solar radiation should contribute to an increased transformer temperature we constrained the coefficients, sc_j, to be positive. The best results, i.e., significant parameters and improved estimations of the transformer temperature, for TRF 1 were achieved using a polynomial degree of three and four splines (i.e. n = 4 in (6)). It was also discovered that the second spline is insignificant and therefore sc_2 was set to a value close to zero. This improved the process of optimizing the parameters in the model. The low significance of the second spline could be due to a shadow effect during the time when the second spline is active. For TRF 2 the best results were achieved with five splines (i.e. n = 5 in (6)) and again by setting sc_2 to a value close to zero.

4.3. Tested models

Many different models were tested and evaluated in the model development process. As it is infeasible to present all models evaluated within this paper, we will discuss a representative sample from the model selection process. This sample includes a one state model, a two state model, an extended two state model and two three state models, where the latter are the final models for TRF 1 and 2, respectively. The overall model selection process followed the same steps for both TRF 1 and 2. However, there was a slight difference in identifying the final three state model.

4.3.1. One state model

As stated in Section 4.1, we used a forward selection process and thus, we started out with a simple model. The initial model had one state and ambient temperature and current as input variables. This was to represent the simplest model using the most relevant inputs according to the correlation analysis in Section 4.2 (solar radiation was ignored here due to reasons described in Section 4.2.2). The system and observation equations are presented below:

$$dT_\mathrm{i} = \frac{1}{C_\mathrm{i}}\left(\Phi_\mathrm{h} + \frac{1}{R_\mathrm{ia}}(T_\mathrm{a} - T_\mathrm{i})\right)dt + \sigma dw \tag{7}$$

$$T_{\mathrm{lid},k} = T_{\mathrm{i},k} + e_k \tag{8}$$

where k are points in time, t_k, of measurements, T_i is the corresponding state to the observed lid temperature T_lid, C_i is the thermal capacitance at the transformer lid, R_ia is the thermal resistance between the lid and the ambient temperature (including the housing) and Φ_h represents the heat generated by the transformer losses. In this model the load and no-load losses were modeled by only using the three-phase current squared as input, i.e. $\Phi_\mathrm{h} = aI^2_\mathrm{3ph} + b$.

The system can also be described by the circuit model in Fig. 4, where the heat generated by load and no-load losses is modeled as a current source and the cooling from ambient temperature as a voltage source.

4.3.2. Two state model

We extended the model by adding a second state for the temperature inside the transformer, T_t. Note that this is an arbitrary point inside the transformer and does not aim to identify the hot-spot temperature, but rather model the heat transfer between the inside of the transformer and the lid, i.e. from T_t to T_i. The system equations and observation equation are:

$$dT_\mathrm{i} = \frac{1}{C_\mathrm{i}}\left(\frac{1}{R_\mathrm{ti}}(T_\mathrm{t} - T_\mathrm{i}) + \frac{1}{R_\mathrm{ia}}(T_\mathrm{a} - T_\mathrm{i})\right)dt + \sigma_1 dw_1 \tag{9}$$

$$dT_\mathrm{t} = \frac{1}{C_\mathrm{t}}\left(\Phi_\mathrm{h} + \frac{1}{R_\mathrm{ti}}(T_\mathrm{i} - T_\mathrm{t})\right)dt + \sigma_2 dw_2 \tag{10}$$

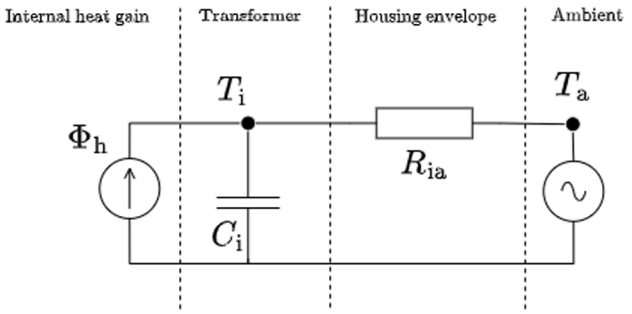

Fig. 4. RC circuit of the one state model *Ti*.

$$T_{\mathrm{lid},k} = T_{\mathrm{i},k} + e_k \tag{11}$$

where k are the points in time, t_k, of measurements, T_t is the thermal state within the transformer and generated heat due to power losses is described by the three-phase current squared ($\Phi_\mathrm{h} = aI^2_\mathrm{3ph} + b$). The Wiener processes are denoted w_1 and w_2 for (9) and (10), respectively. No extra input variables were added in this model compared to the one state model, but parameters for the thermal resistance, R_ti, between the states (T_t and T_i) and capacitance, C_t, for the internal state (T_t) were added. This is also visualized in the circuit model in Fig. 5.

4.3.3. Extended two state model

In this step, we extended the two state model by adding the wind speed as input to the model. This step was done to investigate the impact on the performance of the model that comes with expanding the model through adding inputs rather than adding states to the model. The resulting system and observation equations are as follows:

$$dT_\mathrm{i} = \frac{1}{C_\mathrm{i}}\left(\frac{1}{R_\mathrm{ti}}(T_\mathrm{t} - T_\mathrm{i}) + \frac{1}{R_\mathrm{ia}}(T_\mathrm{a} - T_\mathrm{i}) + \omega\Phi_\mathrm{wind}\right)dt + \sigma_1 dw_1 \tag{12}$$

$$dT_\mathrm{t} = \frac{1}{C_\mathrm{t}}\left(\Phi_\mathrm{h} + \frac{1}{R_\mathrm{ti}}(T_\mathrm{i} - T_\mathrm{t})\right)dt + \sigma_2 dw_2 \tag{13}$$

$$T_{\mathrm{lid},k} = T_{\mathrm{i},k} + e_k \tag{14}$$

where Φ_wind is the wind speed and ω the corresponding parameter. All other variables and parameters are described in Section 4.3.2. The extended two state model is also illustrated in the circuit model in Fig. 6, where the wind speed acts as a current source to the transformer temperature state.

4.3.4. Three state model

In the three state model, we added a hidden state for the temperature, T_b, representing the temperature inside the metal housing, in which the transformer is placed. It was further explored whether more environmental or electrical inputs should be added to the model. Solar radiation was added to the system equations as an environmental input to increase the performance of the model as described in Section 4.2.2. Due to different locations and properties of the two studied transformers, their three state models are presented separately.

Transformer TRF 1

The three state model for TRF 1 is described by (15)–(18).

$$dT_\mathrm{i} = \frac{1}{C_\mathrm{i}}\left(\frac{1}{R_\mathrm{ti}}(T_\mathrm{t} - T_\mathrm{i}) + \frac{1}{R_\mathrm{ib}}(T_\mathrm{b} - T_\mathrm{i})\right)dt + \sigma_1 dw_1 \tag{15}$$

$$dT_\mathrm{t} = \frac{1}{C_\mathrm{t}}\left(\Phi_\mathrm{h} + \frac{1}{R_\mathrm{ti}}(T_\mathrm{i} - T_\mathrm{t})\right)dt + \sigma_2 dw_2 \tag{16}$$

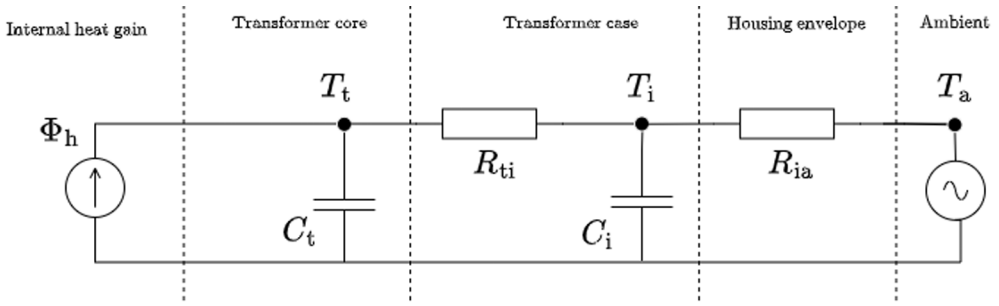

Fig. 5. RC circuit of the two state model *TiTt*.

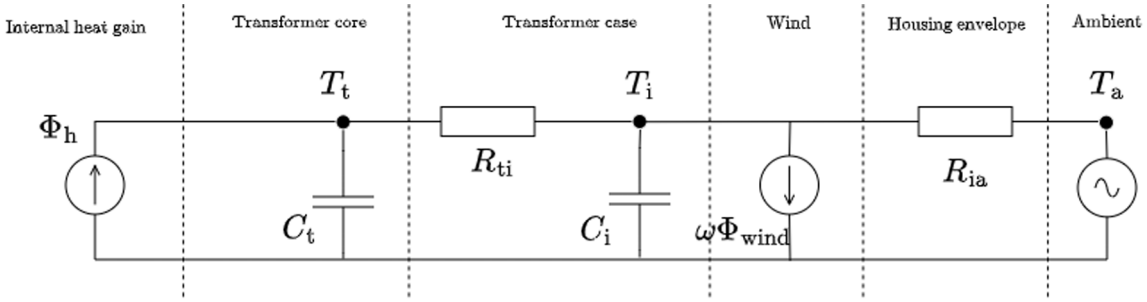

Fig. 6. RC circuit of the two state model *TiTt* with wind contribution.

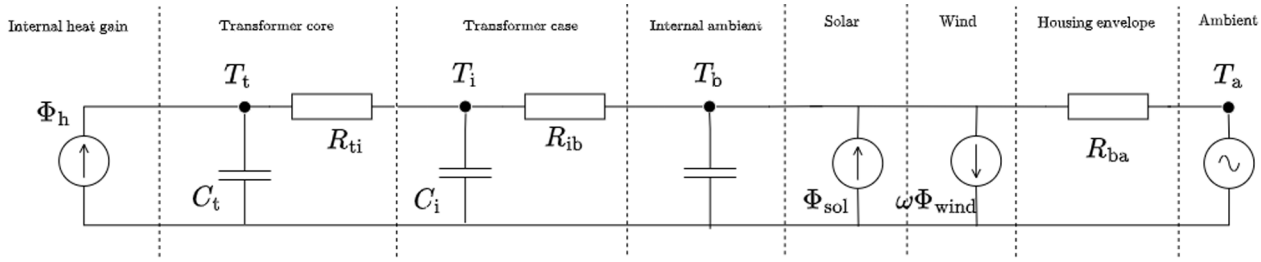

Fig. 7. RC circuit of the three state model *TiTtTb*.

$$dT_b = \frac{1}{C_b}\left(\frac{1}{R_{ib}}(T_i - T_b) + \frac{1}{R_{ba}}(T_a - T_b) + \omega\Phi_{wind} + \Phi_{sol}\right)dt + \sigma_3 dw_3 \tag{17}$$

$$T_{lid,k} = T_{i,k} + e_k \tag{18}$$

where R_{ib} is the thermal resistance between the state at the lid, T_i and the state in the housing, T_b. C_b is the thermal capacitance in the housing, Φ_{sol}, is explained in (6) and Φ_h is described by the three-phase current squared ($\Phi_h = aI_{3ph}^2 + b$). All other variables and parameters are explained in Sections 4.3.2 and 4.3.3. The thermal model for TRF 1 is also depicted in the thermal circuit model (Fig. 7).

Transformer TRF 2

For the final three state model, the neutral current turned out to be a significant input to TRF 2, but not to TRF 1. Thus, for TRF 2, the neutral current was added to Φ_h in both the system Eq. (16) and in the RC circuit in Fig. 7 (i.e. $\Phi_h = aI_{3ph}^2 + b + cI_N^2$).

It should also be noted that the input for solar radiation differs for TRF 1 and 2 as described in Section 4.2.2.

4.4. Temperature estimation and prediction

As described in Section 4.2.1, the power losses are directly causing heating inside the transformer. Meanwhile, the measuring point is at the lid of the transformer (see Fig. 1) and it is realized that there will be a time delay between the time of the hot-spot temperature inside the transformer and corresponding effects seen at the observed transformer lid temperature. This can also be realized by observing the thermal resistance in the oil as well as thermal capacitance in the RC circuits in e.g. Fig. 7.

This time delay is important for the understanding of which prediction horizon of the transformer lid temperature gives an indication of the core conditions at the current time step. To investigate this, a cross-correlation analysis between three-phase current squared and transformer lid temperature was carried out. Assuming that the leakage flux is heating the metallic parts quite instantly, the time span between an increase in current squared and the temperature rise at the lid gives an indication of the time delay. The three-phase current squared was chosen as the main explaining variable for the transformer inner temperature, following the description of transformer losses above and given that it has a higher correlation than the neutral current as seen in Fig. 3. The analysis was done by dividing the time series for each transformer into segments of days. The cross-correlation between the three-phase current squared and transformer lid temperature was calculated, while noting the lag at which the maximum value of the cross correlation was achieved. For TRF 1 the maximum cross correlation occurred on average at a lag of 5 ± 1.5 time steps with a 95% confidence interval. For TRF 2 it instead occurred at 3.5 ± 1 time steps with a 95% confidence interval. Keeping in mind that each time step is 30 min, this means that the heat

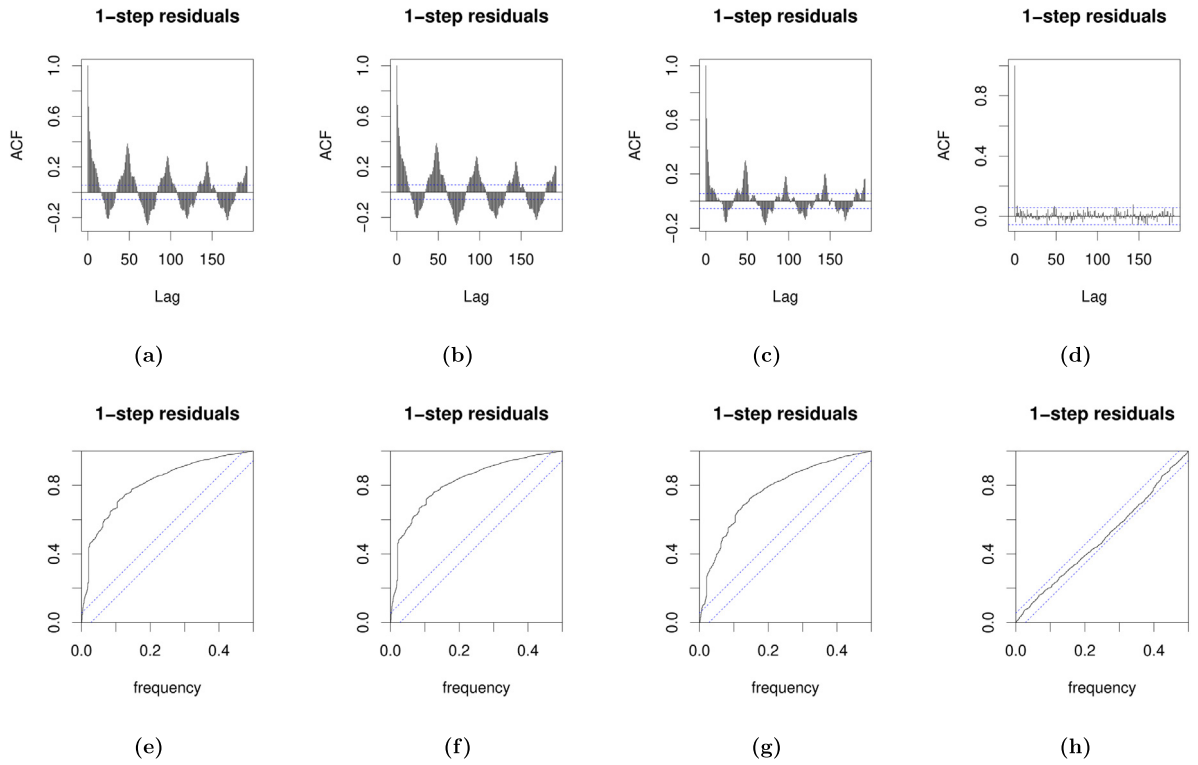

Fig. 8. Residual analysis for the model selection process for transformer 1. Graphs for ACF are shown in subfigures (a)–(d) and cumulated periodogram in (e)–(h). The results for the different models are presented as follows: One state model in (a) and (e), two state model in (b) and (f), extended two state model in (c) and (g), three state model in (d) and (h). Blue dotted lines indicate 95% confidence bands under the assumption that the residuals are white noise.

generated from load losses takes 2.5 ± 0.75 hours to transfer to the measuring point at the lid for TRF 1 and for TRF 2 it takes 1.75 ± 0.5 hours. The difference in time delay between the two transformers is most likely due to the smaller size and thus thermal inertia of TRF 2 (200 kVA), which is half the size of TRF 1 (400 kVA).

As seen in the model application framework in Section 2 (Fig. 1) the DSO should receive predictions such that adjustments can made to the load of the transformer before the limit is violated. Given that predictions at 5 ± 1.5 and 3.5 ± 1 time steps ahead, relate to the current state inside the transformer, predictions further ahead are required to support the DSO in the model application framework. For this purpose we evaluate the thermal model at 12 step ahead predictions (6 h), leaving 3.5 and 4 h respectively to activate flexible resources.

5. Results and discussion

In this section we present and analyze the results from the models defined in Section 4.3. To avoid repetition, the results are mostly discussed for TRF 1, and the models of TRF 2 are presented for the sake of comparison. We further discuss the results in the context of the model application framework presented in Section 2.

5.1. Residual analysis

Based on the definition of the model in (2), the residuals from an adequate model should be in the form of normally distributed white noise. The residual analysis is done by evaluating the auto correlation function (ACF), to ensure that the residuals are independent, and also by looking at the cumulated periodogram, to ensure that no frequencies are left in the residuals. Both evaluations aims to identify whether the residuals are white noise or not. If the residuals are not white noise, there are patterns in the system that the model is not capturing. The principles of using the residuals for a model evaluation are based on the methods suggested in [33].

The ACF and cumulated periodograms from the models presented in Section 4.3 are shown in Fig. 8. It can be seen that the significant and periodic values in the ACF are gradually decreasing throughout the model selection process. However, little improvement is seen between the one and two state models, whereas reduced ACF and a shift in the cumulated periodogram can be seen for the extended two state model. This means that extending the model by adding input variables to the model was necessary. It should be noted that adding states such that the input variables could be described in a physics informed manner was also required and improvements for the residual analysis were observed through such extensions. For the presented one and two state models the ACF has significant periodic values indicating that there are patterns or behaviors in the system that the models do not capture. It is further seen in the cumulated periodograms that some frequencies of the residuals are dominating for these models. Thus, it cannot be concluded that the residuals are white noise and neither the one nor the two state models properly describe the system.

Looking at the residual analysis for the three state model in (15)–(18) for TRF 1, it can be seen that the ACF (Fig. 8(d)) does not have any significant values. Furthermore, the cumulated periodogram (Fig. 8(h)) shows no dominating frequencies in the residuals, but lies within the interval of the 95% confidence interval. Thereby, the three state model gives residuals that are white noise and we conclude that the three state model provides an adequate description of the system.

The ACF and cumulated periodogram for the three state model for TRF 2 show white noise residuals within a 95% confidence

Table 2
Summary of RSS for 1 and 12 step ahead, mean average error and maximum absolute error for 12 step ahead predictions, log likelihood from models for TRF 1 and TRF 2 using the training data set. The computation time of estimating the parameters, using a Intel core i7 @ 1.90 GHz, 16 GB RAM and running on Linux Pop! OS version 21.10, is also presented.

Model	RSS 1 step	RSS 12 step	MAE	Max error	Log likelihood	Computation time
Trf 1: One state	21.6	1035	0.79	3.82	772	11 secs
Trf 1: Two state	21.4	1061	0.81	3.81	718	1.34 mins
Trf 1: Extended two state	16.2	468	0.54	2.54	885	1.84 mins
Trf 1: Three state	8.5	261	0.39	1.69	1273	5.95 mins
Trf 2: One state	50.4	1179	1.06	5.08	−37.6	9 secs
Trf 2: Two state	50.0	1184	1.07	5.05	−34.4	1.34 mins
Trf 2: Extended two state	42.0	654	0.77	4.40	38.9	2.16 mins
Trf 2: Three state	27.6	442	0.63	2.47	212.8	6.37 mins

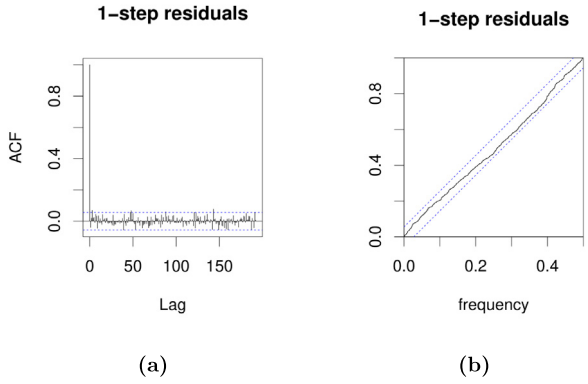

Fig. 9. Residual analysis for the three state model for TRF 2. The ACF is shown in subfigure (a) and cumulated periodogram in (b). Blue dotted lines indicate a 95% significance level.

interval (Fig. 9). Thereby, this three state model with the modification described in Section 4.3 is identified as the final model for TRF 2.

5.2. Residual sum of squares and likelihood analysis

We analyzed the residual sum of squares (RSS) values and mean average error (MAE) to evaluate whether the errors in the output given the observed data were reduced in the model selection process. The values of the log likelihood function were used to compare the models. As shown in Table 2, by moving from one state models to three state models the values of RSS, MAE and likelihood values of both transformers are improved, which confirms an increased performance of the model throughout the selection process. Comparing the results for both transformers shows that the proposed three state model for TRF 1 has a better performance than the three state model for TRF 2. Furthermore, in the final models a maximum absolute error of 1.69 and 2.47 °C was seen for TRF 1 and TRF 2, respectively, using the training data. If instead we use the test data, the maximum absolute errors were 5.6 and 3.0 °C, respectively. For TRF 2 this is acceptable for the application of the dynamic rating framework, which is satisfying given that this transformer is the most critically loaded, with a peak above the nameplate rating. For TRF 1, the results could be improved, but it should be mentioned that the MAEs are 0.73 and 0.87 °C, respectively, and the high maximum error for TRF 1 is an exception.

5.3. Estimated parameters

The estimated parameters for the final model are seen in Table 3 for TRF 1 and 2. Normalized inputs were used for all variables, except for the temperature variables, which were kept in measured °C. If including the squared neutral current, I_N^2, for TRF 1, the estimated parameter, c, obtained a p-value higher than 0.1. Thus, there is a slight difference in the final model for the two transformers, meaning that the neutral current is a significant input variable to TRF 2, whereas it was not for TRF 1. Noting that the percentage of neutral current to total phase current is quite similar for both transformers (13% for TRF 1 and 12% for TRF 2), it is concluded that a higher harmonic content in TRF 2 is probably not the reason for this difference. Instead another possible reason is that TRF 2 has a loading that is almost twice as large as the loading condition for TRF 1 (see Section 3). This could mean that the power related factors have a higher impact compared to environmental factors for TRF 2, and hence, the neutral current is significant during such a loading condition. With the reasoning above, this means that when implementing the model for a transformer with loading at and above nameplate rating, the neutral current should be included as an input variable to the model in accordance with the model in Section 4.3.4. This is to account for the losses due to the neutral current, which is linked to third order harmonics as well as unbalance between the phase currents.

Moreover, different numbers of splines were needed for the two transformers to model the impact from the solar radiation. This is reasonable given that different shading and angle to direct solar radiation could occur depending on the placement of the

Table 3
Parameter estimations and standard deviations (Std. Dev.) in the final models for TRF 1 and 2. All inputs were normalized, except for the initial temperatures, which are presented in °C.

Parameter	TRF 1 Estimate	Std. Dev.	TRF 2 Estimate	Std. Dev.
Initial state T_i	28.5	0.07	28.2	0.15
Initial state T_b	22.7	1.2	20.2	1.9
Initial state T_t	52.0	14.2	41.5	5.1
a	2.61	0.30	3.33	0.26
b	0.607	0.111	0.863	0.113
c	−−	−−	0.158	0.055
C_b	4851	876	2312	403
C_e	412	69	168	40
C_t	413	165	394	79
$ln(\sigma_e^2)$	−45.7	0.09	−45.7	0.07
$ln(\sigma_1)$	−25.1	5.3	−20.7	11.3
$ln(\sigma_2)$	−−	−−	−48.3	26.8
$ln(\sigma_3)$	−5.46	0.12	−4.79	0.14
R_b	3.97	0.79	5.28	0.97
R_{ia}	14.2	1.76	9.76	0.89
R_{ti}	15.8	7.5	8.85	3.08
sc_1	3.67	0.78	14.8	3.64
sc_3	1.86	0.41	1.10	0.60
sc_4	1.03	0.24	1.68	0.58
sc_5	−−	−−	1.41	0.37
ω	−0.817	0.124	−0.902	0.134

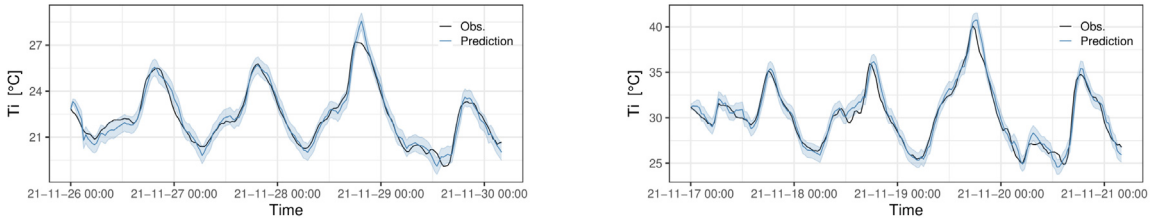

(a) 5 step ahead predictions for the test data set, using the one state model for TRF 1.

(b) 4 step ahead predictions for the test data set, using the extended two state model for TRF 2.

Fig. 10. Predictions of the transformer lid temperature for 5 and 4 time steps ahead, respectively, corresponding to the current state inside the transformer. Black line — observations, Blue line — predictions, Light blue area — 95% PI. (For interpretation of the references to color in this figure legend, the reader is referred to the web version of this article.)

transformers. Identification of the splines could potentially to some extent be automized if the model is applied at large scale. It was, however, seen for both transformers that the solar radiation only had an impact during the morning until noon. Seasonal effects could also be incorporated in the future, as the described interval, solar spline function and effects from the wind would probably change throughout the year. However, to investigate annual seasonal effects, time series of minimum two years are required. Since the model was developed using the available data from November 2021, it was not relevant for this study, but is rather a part of future work. As discussed in Section 3, this time series length was an active choice given the available data set to avoid long-term seasonal effects. However, as later reported in Section 5.4, the data set was sufficient given the selected grey-box modeling approach to provide good prediction results on the test data.

Although four different temperature measurements were available (see Fig. 1), the best results were achieved using only one of them (T_{lid}). This further reduces the number of sensors required in the installation in order to apply the model.

5.4. Application of the proposed method for real time estimation and prediction

As described in Section 4.4, predictions at 5 ± 1.5 and 3.5 ± 1 time steps ahead relate to the current state inside the transformer. The time delay is due to the time constants of the system and the predictions at these horizons are useful for control room purposes. Therefore, we evaluated the predictions at horizons 5 and 4 (rounded off from 3.5) time steps ahead, or 2.5 and 2 h, respectively. The predictions and PIs can be seen in Fig. 10. Since Gaussian white noise residuals were proven in the residual analysis in Section 5.1, 95% PI's assuming Gaussian errors could be computed using CTSM-R. Furthermore, the predictions and predictions intervals are constructed using collected data for the input variables. The predictions follow the observations for most of the time. Nevertheless, there is an overshoot in the estimation of the evening peak on the 28th of November. This could be due to "the memory" (the derivative of previous time steps) in the model structure and the previous positive trend in the temperature time series. Although the prediction intervals do not fully capture the observations, they give reasonable predictions of the states. Taking in to account that there is a 95% PI in the graph, under and over estimations will occur from time to time. Through adjusting the PIs, the likelihood of having an observation outside the PIs can be as small as desired. Thereby, the DSO can account for the uncertainty in their control strategies by adjusting the PIs. Predictions further ahead than the current state are required to support the DSO in the model application framework in Fig. 1. We therefore evaluated 12 step ahead predictions (6 h), giving 3.5 and 4 h respectively to adjust the power flow through activating flexible resources.

The 12 step ahead predictions for the test data set are presented in Fig. 11. Improvements in the accuracy of the prediction and the prediction intervals (PIs) can be seen as the model is expanded from one to three states. For the one and two state models the PI often misses the observation, which is a sign of a not well enough implemented model. For the final three state model for both transformers, the observations are, however, most of the time inside the PIs. Naturally, some observations will be outside of the PI due to the 95% significance level of the PIs. Most importantly for the safety of the grid operation, the PIs capture the peaks of the temperature, which are the most critical points for the implementation. Thus, we conclude that the predictions at this time horizon are fulfilling the requirements for usage in the model application framework.

Nevertheless, there is also potential for improvements to reduce the uncertainty of the model. The model is developed for, and using data from, normal cyclic operation. However, if the model should be applied under other operating conditions, such as long time emergency loading [2], a reduced uncertainty might be required. For instance, heat run tests could be performed to establish a model, table or other approaches, that can estimate the hot-spot temperature given the transformer lid temperature and loading conditions. This could, for example, be done with optical sensors, which could also be utilized for model validation. With the proposed model, the DSO would need to establish some extra temperature margin that is acceptable from a safety point of view given the uncertainty. Performing such tests would reduce this margin as DSOs would have more knowledge on how to translate the transformer temperature and loading condition to possible scenarios for the hot-spot temperature.

Furthermore, other improvements, such as adding more states to the model, could be investigated. This could, for example, include seasonal effects from solar radiation or having adaptive parameters. It should, however, be noted that such improvements in the accuracy could have a negative impact on the computation time. As seen in Table 2 the computational time increased when increasing the model order.

5.5. Comparison to state-of-the-art

The proposed method in this paper is based on k–step ahead predictions. We have especially focused on evaluating the model at a prediction horizon of 6 h, i.e. $k = 12$. The method is designed such that it can be installed on transformers in service without power delivery interruption through the usage of non-intrusive measurements. Thereby, the engineering of this method is considerably different from that found in the-state-of-the-art. Despite these differences this section discusses and compares the proposed model to other models found in literature.

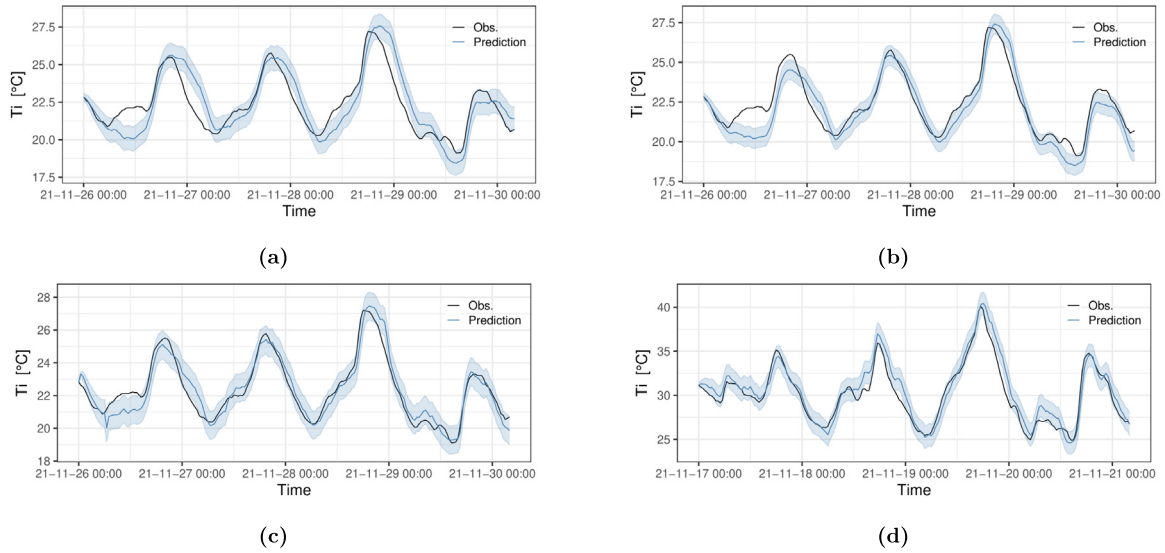

Fig. 11. Prediction analysis for 12 step ahead (6 h) predictions. Subfigures (a)–(c) show predictions for TRF 1 using the one state model (a), extended two state model (b) and the final three state model (c). Subfigure (d) shows predictions for TRF 2 using the final three state model. Black line — observations, Blue line — predictions, Light blue area — 95% PI. (For interpretation of the references to color in this figure legend, the reader is referred to the web version of this article.)

In both IEC Std. 60076-7 and Annex G of the IEEE C57.91 Standard, the thermal models consider the top-oil temperature in the tank, whereas the proposed method is based on the temperature measured on the top of the transformer. Although the measured temperature is linked to the top-oil temperature, the two temperatures cannot be compared directly in quantitative measures. Furthermore, the proposed model is designed to deliver temperature forecasts ahead in time, while the thermal models in the standards are deterministic models better suited for monitoring purposes. For the intended application, the proposed model has a clear advantage as opposed to the standard models, since no sensors are needed inside the transformer, which allows for a non-intrusive application in existing DSO grids. This feature is also advantageous in comparison to other dynamic rating models using in tank measurements as inputs to their models (e.g. [7]).

Some models have been found in literature that allows for a quantitative comparative analysis. For instance, in [34] the authors report a root mean squared error (RMSE) of 0.7 °C for their fuzzy tree method, predicting winding hot-spot temperature. Another example is [11], which proposes a new thermal method for average winding and hot-spot temperature, which outperforms the method in Annex G of the IEEE C57.91 Standard. The authors report squared average errors of 1.26 and 1.36 °C for the two proposed methods as well as maximum errors of 5.54 and 4.42 °C, respectively. These measures can be compared to results of the proposed model reported in Section 5.2, which gives MAE of 0.39 and 0.63 °C for TRF 1 and 2, respectively, and maximum error of 1.69 and 2.47 °C. Nevertheless, the reported errors from the proposed model are for 6 h ahead predictions whereas the two aforementioned studies are rather monitoring or real-time estimation errors. Furthermore, the two studies consider temperatures which require measurements inside the transformer. In [19], a very low RMSE of 0.03–0.08 °C is reported for their hot-spot prediction model. However, their proposed method is for a dry-type transformer and is also not a k–step ahead model, but rather a monitoring model. Looking at the existing literature, it is thus concluded that the results of the proposed model are very good in terms of accuracy. However, due to the unique engineering setup of the proposed model it is difficult to perform a more detailed comparative analysis.

Moreover, it is relevant to compare the proposed model to black-box models in literature. In [17], the authors used an artificial neural network to predict the temperature distribution of dry-type transformers and achieves a mean squared error of 2.71%. The study uses a large data set and involves 3D data, considering temperature distribution for monitoring purposes and is intended for transformer designing purposes, which makes the studied case suitable for applying black-box approaches. Another example is found in [35], where the authors use nonlinear autoregressive neural networks and support vector machines for thermal modeling of high rating transformers (180–1000 MVA). The purpose of their study was to monitor the transformer condition and a RMSE of 1.6 °C is reported for their final model. Although our proposed model partially uses non-parametric and data driven methods, it was not relevant to rely on a purely data-driven black-box method, since it would require a much larger data set with longer time series for both model development and testing. Instead, the proposed model can be applied with shorter time series and parameters in the model can be re-optimized as more data becomes available. Furthermore, the mentioned studies concerns transformer monitoring purposes, for which black-box models are suitable as model calibration can occur continuously. The purpose of our model is to provide k–step ahead predictions as well as estimates of the uncertainty of the predictions and in this case it is not suitable to design the model without any physics information. Furthermore, models based on partial physical information are often more robust than pure black-box models [28,36].

5.6. Discussion on applicability of the model

To evaluate the applicability of the thermal model, the computation time is a crucial factor. It should be noted that although capturing non-linear behavior, such as heating from the solar radiation, the grey-box models are formulated as linear models. This reduces the computational burden of optimizing the parameters in the models. As seen in Table 2, the computation time increases with increasing order of the model. It is also seen that the time to run and optimize the parameters for the final model is approximately six minutes for TRF 1 and 2, respectively. With this computation time, the model can be updated on a regular basis, enabling the usage of the model in grid operation. How often the parameters of the model should be updated is a compromise between model accuracy and computational burden. It is possible to update the parameters for every time step given

that the time resolution is 30 min, but it needs to be evaluated if that is feasible. The DSO has to weight the gained capacity from having an accurate thermal model against the economical cost of updating the models, taking into account how many transformers in the system the model will be applied to.

Given the analysis of the predictions, accuracy and the computational time, the model can be applied for online forecasting of the transformer temperature in distribution grid operation. Due to the ability to provide predictions the model can be used for warning and control purposes. The manufacturer of the transformer in this study also claims that keeping track of the transformer lid temperature should be enough to safely operate the transformer. The engineering setup for model application includes sensors, which are non-intrusive, load and weather data and data communication to collect these data sets. However, for full implementation of the model application framework, an algorithm for the online forecasting tool needs to be developed. This involves re-optimizing the parameters at an appropriate frequency and to automate the optimization of B-splines (see Section 5.3) to fully generalize the model.

In this work we have also found a solution that is both affordable and practical in terms of hardware installation. This is due to the limited number of input variables required to run the models. Weather data can be fetched from the meteorological forecast provider (in our case DMI) and current sensors have become more affordable in recent years. Furthermore, the model automatically includes environmental and electrical characteristics specific to the transformer, potentially unlocking even more capacity than a deterministic solution based on standard conditions. Since we have a stochastic model, we can also provide PIs accounting for the uncertainty.

The model could potentially be extended to higher rating MV/LV transformers, provided that data for such transformers becomes available. As the leakage flux increases with increasing size, electrical input variables will most likely have a larger comparative impact and the model structure for TRF 2 would be recommended for initial model calibration to be reduced if necessary.

6. Conclusion

In this paper, we proposed a framework for obtaining dynamic rating of transformers in power distribution grids. For this purpose, we developed a thermal model for estimating and predicting transformer temperature. The model was developed using data from a real world experimental installation and can be used for developing an online monitoring and forecasting algorithm for DSOs.

The proposed model is formulated as a grey-box model. This is a physics-informed data-driven model which is optimized for assimilating information from sensors into the model parameters. Furthermore, this approach gives a possibility for providing prediction intervals, and hereby we can specify the risk of violating the temperatures.

The identified input variables in the proposed thermal models result in an affordable and practical solution. The hardware in the solution can be installed without interruption of power supply and without exchanging any equipment.

Furthermore, the proposed thermal model has been proven to give reasonable estimations and predictions. This enables the ability to operate the transformer dynamically, unlocking unused capacity at certain times.

The proposed model also accounts for the electrical and environmental conditions at a specific transformer. This could give a more specifically applied DTR, unlocking more capacity than a DTR or thermal model based on standard conditions.

Moreover, the computational time for the model gives the option to update the parameters of the model on a regular basis. This further enables implementation in grid operation as the accuracy can be maintained.

6.1. Future work

Although the proposed model can be applied for online monitoring and forecasting as it is, it could be complemented or improved to reduce the uncertainty.

As discussed in Section 5, heat run tests with optical sensors should be made to establish how the transformer lid temperature and loading conditions affect the hot-spot temperature and to further validate the model. This could provide a better insight into the transformer hot-spot temperature. Moreover, in future studies the model should be evaluated for higher rating transformers.

Expansions to the model, such as states for seasonal effects, adaptive parameters or improved local weather forecasts could be developed. However, caution needs to be taken to not increase the computation time and burden too much or alternatively find a workaround that does not require us to rerun the model to update the parameters. We are planning on collecting data continuously during the coming years, and within a few years we aim at formulating an extension of the models which includes seasonal effects.

Finally, an algorithm that uses the proposed model and input data to deliver the forecasts online in real time needs to be developed for full implementation of the concept.

CRediT authorship contribution statement

E.M.V. Blomgren: Conceptualization, Project administration, Software, Visualization, Formal analysis, Investigation, Methodology, Writing – original draft. **F. D'Ettorre:** Methodology, Investigation, Validation, Visualization, Writing – original draft. **O. Samuelsson:** Conceptualization, Supervision, Writing – review and editing. **M. Banaei:** Writing – original draft, Visualization. **R. Ebrahimy:** Supervision, Writing – review and editing. **M.E. Rasmussen:** Methodology, Formal analysis, Visualization. **N.H. Nielsen:** Methodology, Formal analysis, Visualization. **A.R. Larsen:** Methodology, Formal analysis, Visualization. **H. Madsen:** Conceptualization, Writing – review and editing, Supervision, Funding acquisition.

Declaration of competing interest

The authors declare that they have no known competing financial interests or personal relationships that could have appeared to influence the work reported in this paper.

Data availability

The authors do not have permission to share data

Acknowledgments

This work was supported by the Flexible Energy Denmark (FED) project funded by Innovation Fund Denmark under Grant No. 8090-00069B and Ebalanceplus project funded by the European Union's Horizon 2020 under the grant agreement number of 864283. The authors also would like to thank Claus Schack Urup for technical support and providing the data for this study.

References

[1] A.A. Taheri, A. Abdali, M. Taghilou, H. Haes Alhelou, K. Mazlumi, Investigation of mineral oil-based nanofluids effect on oil temperature reduction and loading capacity increment of distribution transformers, Energy Rep. 7 (2021) 4325–4334, http://dx.doi.org/10.1016/j.egyr.2021.07.018.

[2] IEC, DS/IEC 60076-7:2018, power transformers – part 7 : Loading guide for mineral-oil-immersed power transformers, 2018.

[3] IEEE Standards Board, IEEE Standard Test Code for Liquid-Immersed Distribution, Power and Regulating Transformers Std C57.12.90, IEEE, 1999.

[4] M.F. Lachman, P.J. Griffin, W. Walter, A. Wilson, Real-time dynamic loading and thermal diagnostic of power transformers, IEEE Trans. Power Deliv. 18 (1) (2003) 142–148, http://dx.doi.org/10.1109/TPWRD.2002.803724.

[5] K. Morozovska, P. Hilber, Study of the monitoring systems for dynamic line rating, Energy Procedia 105 (2017) 2557–2562, http://dx.doi.org/10.1016/j.egypro.2017.03.735.

[6] C.J. Wallnerström, P. Hilber, P. Söderström, R. Saers, O. Hansson, Potential of dynamic rating in Sweden, in: 2014 International Conference on Probabilistic Methods Applied to Power Systems, PMAPS 2014 - Conference Proceedings, IEEE, 2014, http://dx.doi.org/10.1109/PMAPS.2014.6960605.

[7] T.S. Jalal, N. Rashid, B. Van Vliet, Implementation of dynamic transformer rating in a distribution network, in: 2012 IEEE International Conference on Power System Technology, POWERCON 2012, IEEE, 2012, pp. 2–6, http://dx.doi.org/10.1109/PowerCon.2012.6401328.

[8] T. Zarei, K. Morozovska, T. Laneryd, P. Hilber, M. Wihlén, O. Hansson, Reliability considerations and economic benefits of dynamic transformer rating for wind energy integration, Int. J. Electr. Power Energy Syst. 106 (2018) 598–606, http://dx.doi.org/10.1016/j.ijepes.2018.09.038.

[9] F. Josue, I. Arifianto, R. Saers, J. Rosenlind, P. Hilber, Suwarno, Transformer hot-spot temperature estimation for short-time dynamic loading, in: Proceedings of 2012 IEEE International Conference on Condition Monitoring and Diagnosis, CMD 2012, IEEE, 2012, pp. 217–220, http://dx.doi.org/10.1109/CMD.2012.6416414.

[10] A. Arabul, I. Senol, Development of a hot-spot temperature calculation method for the loss of life estimation of an ONAN distribution transformer, Electr. Eng. 100 (2018) http://dx.doi.org/10.1007/s00202-017-0641-0.

[11] C. Gezegin, O. Ozgonenel, H. Dirik, A monitoring method for average winding and hot-spot temperatures of single-phase, oil-immersed transformers, IEEE Trans. Power Deliv. 36 (5) (2021) 3196–3203, http://dx.doi.org/10.1109/TPWRD.2020.3035842.

[12] S. Taheri, H. Taheri, I. Fofana, H. Hemmatjou, A. Gholami, Effect of power system harmonics on transformer loading capability and hot spot temperature, in: 2012 25th IEEE Canadian Conference on Electrical and Computer Engineering: Vision for a Greener Future, CCECE 2012, IEEE, 2012, http://dx.doi.org/10.1109/CCECE.2012.6334834.

[13] B. Das, T.S. Jalal, F.J.S. McFadden, Comparison and extension of IEC thermal models for dynamic rating of distribution transformers, in: 2016 IEEE International Conference on Power System Technology, POWERCON 2016, IEEE, 2016, pp. 1–8, http://dx.doi.org/10.1109/POWERCON.2016.7753896.

[14] Z. Huang, Y. Zhang, Y. Jing, M. Fu, G. Wang, R. Zhuo, Q. Wang, Study on the influence of harmonics on the magnetic leakage field and temperature field of 500 kv connected transformer, in: ICEMPE 2019 - 2nd International Conference on Electrical Materials and Power Equipment, Proceedings, IEEE, 2019, pp. 596–600, http://dx.doi.org/10.1109/ICEMPE.2019.8727246.

[15] I. Kapetanović, J. Hivziefendić, M. Tešanović, Different approaches for analysis of harmonics impact on the transformer losses and life expectancy, in: Lecture Notes in Networks and Systems, vol. 28, 2018, pp. 392–408, http://dx.doi.org/10.1007/978-3-319-71321-2_36.

[16] J. Zhang, L. Cheng, H. Wen, C. Liu, J. Hao, Z. Li, Simulation analysis of the influence of harmonics current on the winding temperature distribution of converter transformer, in: Proceedings - 2021 6th Asia Conference on Power and Electrical Engineering, ACPEE 2021, 2021, pp. 1566–1571, http://dx.doi.org/10.1109/ACPEE51499.2021.9436944.

[17] E.A. Juarez-Balderas, J. Medina-Marin, J.C. Olivares-Galvan, N. Hernandez-Romero, J.C. Seck-Tuoh-Mora, A. Rodriguez-Aguilar, Hot-spot temperature forecasting of the instrument transformer using an artificial neural network, IEEE Access 8 (2020) 164392–164406, http://dx.doi.org/10.1109/ACCESS.2020.3021673.

[18] A. Bracale, P. Caramia, G. Carpinelli, P. De Falco, SmarTrafo: A probabilistic predictive tool for dynamic transformer rating, IEEE Trans. Power Deliv. 36 (3) (2021) 1619–1630, http://dx.doi.org/10.1109/TPWRD.2020.3012180.

[19] Y. Sun, G. Xu, N. Li, K. Li, Y. Liang, H. Zhong, L. Zhang, P. Liu, Hotspot temperature prediction of dry-type transformers based on particle filter optimization with support vector regression, Symmetry 13 (8) (2021) http://dx.doi.org/10.3390/sym13081320.

[20] D.P. Rommel, D. Di Maio, T. Tinga, Transformer hot spot temperature prediction based on basic operator information, Int. J. Electr. Power Energy Syst. 124 (2021) 106340, http://dx.doi.org/10.1016/j.ijepes.2020.106340, URL https://www.sciencedirect.com/science/article/pii/S014206152030867X.

[21] L. Zhang, W. Zhang, J. Liu, T. Zhao, L. Zou, X. Wang, A new prediction model for transformer winding hotspot temperature fluctuation based on fuzzy information granulation and an optimized wavelet neural network, Energies 10 (12) (2017) http://dx.doi.org/10.3390/en10121998, URL https://www.mdpi.com/1996-1073/10/12/1998.

[22] Flexible energy Denmark, 2022, visited on 2022-03-03 URL https://www.flexibleenergydenmark.dk/.

[23] Uni-lab.dk, living labs, 2022, visited on 2022-03-03 URL https://www.uni-lab.dk/en/living-labs/.

[24] DMI, Danish meteorological institute - open data, 2022, visited on 2022-03-03 URL https://confluence.govcloud.dk/display/FDAPI.

[25] P. Nystrup, H. Madsen, E.M.V. Blomgren, G. de Zotti, Clustering commercial and industrial load patterns for long-term energy planning, Smart Energy 2 (2021) 100010, http://dx.doi.org/10.1016/j.segy.2021.100010.

[26] P. Bacher, H. Madsen, Identifying suitable models for the heat dynamics of buildings, Energy Build. 43 (7) (2011) 1511–1522, http://dx.doi.org/10.1016/j.enbuild.2011.02.005.

[27] R. Juhl, J.K. Møller, H. Madsen, ctsmr - continuous time stochastic modeling in R, 2016, arXiv, URL http://arxiv.org/abs/1606.00242.

[28] N.R. Kristensen, H. Madsen, S.B. Jørgensen, Parameter estimation in stochastic grey-box models, Automatica 40 (2) (2004) 225–237, http://dx.doi.org/10.1016/j.automatica.2003.10.001.

[29] IEEE, IEEE STD C57.110-1998 recommended practice for establishing transformer capability when supplying nonsinusoidal load currents, Standard (1998) URL http://ieeexplore.ieee.org/iel5/59/10801/x0247870.pdf.

[30] Z.L. Zhang, H. Zhao, Q. Xin, J. Ye, D.P. Xiao, W. He, A novel neutral current control scheme for three-phase four-wire distribution transformers, Austr. J. Electr. Electron. Eng. 10 (2) (2013) 191–198, http://dx.doi.org/10.7158/E11-081.2013.10.2.

[31] J.B. Noshahr, M. Bagheri, M. Kermani, The estimation of the influence of each harmonic component in load unbalance of distribution transformers in harmonic loading condition, Proceedings - 2019 IEEE International Conference on Environment and Electrical Engineering and 2019 IEEE Industrial and Commercial Power Systems Europe, EEEIC/I and CPS Europe 2019 (2019) http://dx.doi.org/10.1109/EEEIC.2019.8783488.

[32] C. Rasmussen, L. Frölke, P. Bacher, H. Madsen, C. Rode, Semi-parametric modelling of sun position dependent solar gain using B-splines in grey-box models, Sol. Energy 195 (November 2019) (2020) 249–258, http://dx.doi.org/10.1016/j.solener.2019.11.023.

[33] H. Madsen, Time Series Analysis, Chapman and Hall/CRC, 2007, http://dx.doi.org/10.1201/9781420059687.

[34] Y. Zhang, L. Shan, J. Yu, H. Lv, Transformer winding hot spot temperature prediction based on ϵ -fuzzy tree, IOP Conf. Ser. Earth Environ. Sci. 300 (4) (2019) http://dx.doi.org/10.1088/1755-1315/300/4/042034.

[35] A. Doolgindachbaporn, G. Callender, P. Lewin, E. Simonson, G. Wilson, Data driven transformer thermal model for condition monitoring, IEEE Trans. Power Deliv. 37 (4) (2022) 3133–3141, http://dx.doi.org/10.1109/TPWRD.2021.3123957.

[36] T. Hauge Broholt, M. Dahl Knudsen, S. Petersen, The robustness of black and grey-box models of thermal building behaviour against weather changes, Energy Build. 275 (2022) 112460, http://dx.doi.org/10.1016/j.enbuild.2022.112460.